Taylor & Francis
Taylor & Francis Group

SEPARATION SCIENCE AND TECHNOLOGY

Separation Science and Technology

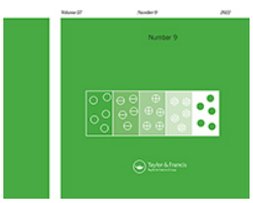

ISSN: (Print) (Online) Journal homepage: https://www.tandfonline.com/loi/lsst20

# Molecularly imprinted composite discs for transferrin recognition

Gülgün Aylaz, Okan Zenger, Gözde Baydemir Peşint & Müge Andaç

**To cite this article:** Gülgün Aylaz, Okan Zenger, Gözde Baydemir Peşint & Müge Andaç (2022) Molecularly imprinted composite discs for transferrin recognition, Separation Science and Technology, 57:9, 1359-1375, DOI: 10.1080/01496395.2021.1990950

**To link to this article:** https://doi.org/10.1080/01496395.2021.1990950

SEPARATION SCIENCE AND TECHNOLOGY
2022, VOL. 57, NO. 9, 1359–1375
https://doi.org/10.1080/01496395.2021.1990950

Taylor & Francis
Taylor & Francis Group



# Molecularly imprinted composite discs for transferrin recognition

Gülgün Aylaz[a], Okan Zenger[b]*, Gözde Baydemir Peşint[b], and Müge Andaç[c]

[a]Nanotechnology and Nanomedicine Division, Institute of Science, Hacettepe University, Ankara, Turkey; [b]Department of Bioengineering, Adana Alparslan Türkeş Science and Technology University, Adana, Turkey; [c]Department of Environmental Engineering, Hacettepe University, Ankara, Turkey

**ABSTRACT**

Human Transferrin (HTr) imprinted composite cryogel (HTr-MIPCC) discs were synthesized with distinctive structure and increased adsorption capacity and specificity for HTr by combining the advantages of the surface imprinting technique. HEMA-based cryogel was embedded with HTr-surface imprinted particles. Thanks to the imprinted particles embedding, both the higher surface area and specific recognition are provided. The structure of the HTr-MIPCC was characterized by FTIR Spectrometer, SEM, swelling studies, flow dynamics, and surface area measurements. The addition of surface imprinted particles into the cryogel disc has resulted in an increased surface area, enhancing the capacity of composite cryogel for HTr adsorption up to 10.96 mg/g and gel fractionation yields reached up to 83%. Selectivity studies were carried out against HIgG and HSA as competitors. The HTr-MIPCC discs were packaged into an FPLC column for selective depletion of HTr. It was calculated that the HTr-MIPCC is 1.071 and 1.062 times selective for HTr than HSA and HIgG, respectively. According to FPLC studies HTr-MIPCC can be considered as an excellent alternative for affinity matrixes used for the detection and selective recognition of HTr directly from human serum. HTr-MIPCC discs can be used several times without any noteworthy reduction in the adsorption capacity of HTr.

**ARTICLE HISTORY**
Received 24 June 2021
Accepted 4 October 2021

**KEYWORDS**
Molecular imprinting; composite discs; chromatography application; transferrin; protein recognition

## Introduction

Human serum transferrin (HTr) is a plasma glycoprotein that coordinates the level of ferric ion ($Fe^{3+}$) in the human body, reversibly binding to ferric ion and transporting it to cells via receptor-mediated endocytosis.[1–3] Owing to the ability of HTr molecule to bind to ferric ions with relatively high affinity, there are not many free ferric ions in the body as HTr binds to most of them. HTr plays an important role as the most crucial ferric pool in humans. It delivers ferric ions throughout the body, taking the advantage of the blood circulation, to various tissues such as the liver, bone marrow, etc.[1,4] Functions of HTr include making free $Fe^{3+}$ soluble at neutral pH; delivering and transferring iron to all the various biological tissues between sites of absorption, utilization, and storage,[2,4,5] preventing the reactive oxygen species to occur.[6] HTr molecule, in addition to other functions, takes part in the defense mechanism of the body.[7] The binding of HTr to iron restricts bacterial growth and survival, therefore decreases during inflammation, leading to an important role as a biomarker for inflammation.[7,8] HTr is one of the high abundant proteins in human blood, the clinical reference value of HTr is 204–360 mg/dL in human blood.[8] It is essential to deplete high abundant proteins (HTr, Human Serum Albumin (HAS), Human Immunoglobulin G (HIgG), etc.) from human serum for proteomic studies, but the complexity of human plasma raises many analytical challenges.[9] It is known that biomarkers used in the diagnosis of diseases, during treatment, and in disease monitoring processes are found in low concentrations. Since very few proteins/biomarkers serve proteomic studies and their signals are masked by high abundant other proteins, major serum proteins need to be removed before analysis. Therefore, it is not surprising that as the first step in protein fractionation procedures, high-abundance protein removal methods have been developed from high-protein body fluids, such as human plasma/serum, cerebrospinal fluid, saliva, and urine.[10–12]

Molecular imprinting is a technique that utilizes a template molecule to construct template-specific binding cavities.[13,14] In recent years, there has been an increasing interest in molecularly imprinting technology compared to traditional methods (antibody, enzymes, specific other biological molecular recognition, etc.).[15,16] In this technique, the specificity of

**CONTACT** Müge Andaç andac@hacettepe.edu.tr Department of Environmental Engineering, Hacettepe University, Ankara, Turkey
*These authors contributed equally.

a polymeric system to its template is based on the physical, chemical, and geometrical properties of the template molecule imprinting process basically consists of the following steps; 1) complex formation between the template molecule (i.e., HTr) and a ligand, 2) polymerization of the template-ligand complex, 3) template removal and formation of template-specific cavities.[13,17] Molecularly imprinted polymers (MIPs) are known to protect their structure even under extreme physical conditions and can be reused plenty of times without any obvious reduction in their ability to capture the molecule of interest.[13,18–20] They are cheaper to produce on large scale with a relatively higher yield, compared to other affinity techniques.[13] The surface imprinting technique has been used in order to improve the adsorption capacity of MIPs, extinguishing the limitations of non-composite MIPs such as the problems with mass transfer and template removal processes.[21] HTr, for example, is a large molecule[3] and it can be encountered in diffusion problems in any separation process of HTr.

Cryogels are affinity gels synthesized at temperatures below 0°C via cryotropic gelation process and owing to their perfect spongy morphology and supermacroporous structure, which makes it possible to study with viscous fluids, such as milk and blood without blocking the column,[22] they draw attention by their relatively reduced flow resistance, shorter diffusion distance, and so on features for both adsorption and desorption processes.[23]

Cryogels are widely used in regenerative medicine, tissue engineering, drug delivery systems, biomedical, diagnostic, therapeutic, biotechnological, and pharmaceutical studies, as they swell easily and allow fluid exchange in their macroporous structures. In addition, cryogels are frequently used in tissue engineering research because of their highly porous structure and hydrophilicity, allowing cell attachment and high mechanical strength. Cryogels have a three-dimensional structure suitable for cell proliferation. Especially, the surface properties of the support materials used in tissue engineering greatly affect the cell affinity.[24] Thanks to the interconnected macropores of cryogels, it provides ease of working with viscous biological fluids. Especially in recent years, there has been a great increase in the number of studies using cryogels for the purification of natural source proteins. Cryogels are more elastic and spongy than other solid monoliths, thanks to interconnected super macropores. In this way, enzymes, nucleic acids, proteins, and even carbohydrates can be easily purified without back pressure problems and diffusion restriction thanks to the interconnected super macropores.[25]

In the study of Pitek et al. (2012), polystyrene nanoparticles functionalized with HTr have been reported. In this technique, HTr molecules were immobilized onto conventional polystyrene nanoparticles using physical adsorption and covalent binding. Synthesized materials have been intended to be used for the stability of HTr in human plasma. This study is lacking a desorption method, in fact, it would be quite harder to perform a desorption experiment when required, since the interactions were covalent.[26]

In the study of Li et al. (2013), transferrin-imprinted polymer particles were synthesized by a hierarchical strategy that is based on three steps: immobilization of transferrin on silica beads, introducing polymer solution into silica beads, and removal of silica matrix and transferrin, resulting in the formation of transferrin-imprinted particles. The binding capacity of the transferrin-imprinted particles is 6.3 mg of protein per gram of material, and the time required to reach adsorption equilibrium was less than 10 min. The imprinting factor of transferrin is approximately 3.3 in the presence of ribonuclease B, cytochrome c, and β-lacto globulin.[27]

In another study, magnetic poly-glycidyl methacrylate-based microspheres have been functionalized with anti-transferrin antibodies. Immobilization has been achieved in the presence of $Fe_3O_4$ nano-powder. Adsorption capacity from artificial plasma was found to be 0.12 mg/g for transferrin. As a result, it can be concluded that the adsorbent prepared can provide specific transferrin separation from protein mixtures in one step, the magnetic properties allow the use of a magnetic separator and the study is promising for the transferrin purification in magnetic fluid beds. These materials, however, are not economically favorable as compared to composite cryogels, and the study is lacking adsorption directly from human serum.[28]

Magnetic fluorescent MIP nanoparticles (FMINPs) were synthesized in order to use in fluorescence detection and isolation of HTr. After the optimization of experimental conditions, FMINPs showed excellent performance for the detection and extraction of HTr (analytical range from 0.025 to 0.175 mg/mL, R-squared value 0.998; minimum limit of detection 0.0075 mg/mL). HTr, bovine hemoglobin, ovalbumin, bovine serum albumin, γ-globin, horseradish peroxidase, and myoglobin solution (each 0.1 mg/mL) were used to detect the selectivity of synthesized materials. FMINPs showed high selectivity against competitors. However, the fluorescence attenuation signals used for the quantification of protein without a linear curve is the drawback of FMINPs. The material needs to be improved with fluorescence boost signals so as to use in the quantitative analysis of protein.[29]

In another study, Zhang et al. (2018) synthesized magnetic molecularly imprinted nanoparticles (deep eutectic solvent-molecular imprinting polymers [DES-MIPs]) with a deep eutectic solvent (DES) from choline chloride and acrylic acid as a functional monomer to specifically recognize and separate HTr in human serum. The DES-MIP has a good adsorption capacity for HTr after optimizing the adsorption conditions and the material was successfully applied in human serum for HTr separation. The maximum adsorption capacity (Qmax) and dissociation constant KL of the MIP by the Langmuir adsorption curve ($R^2$ = 0.9949) were 37.5 mg/g and 0.015 g/L, respectively. HTr, bovine hemoglobin, ovalbumin, bovine serum albumin, and myoglobin (0.15 g/L each) were prepared to evaluate the selectivity of the DES-MIPs. The imprinting factor of the MIP was found to be 3.50 with a relative standard deviation (5.63%). According to results, it was demonstrated that DES-MIPs showed much higher adsorption capacity for HTr compared with other proteins and DES-NIPs had low adsorption for all the proteins.[30]

Miao et al. (2018) have prepared a novel phosphorescent mesoporous microsphere via surface imprinting technique for the detection of transferrin directly from bodily fluids. The dependence of the diameter of surface imprinted microspheres on the capacity of specific transferrin recognition and room-temperature phosphorescence (RTP) signals for highly specific recognition of transferrin was investigated in this study. The analytical range was from 0.05 μM to 1.0 and the lower detection limit was calculated as 0.014 μM. In addition, the imprinting factor for the detection of transferrin was found to be and 3.09 at pH 7.4.[31]

In the study of Çetin and Denizli (2019), microcryogels were synthesized via molecular imprinting technique as artificial antibodies for use in HTr purification. Adsorption and selectivity studies were carried out under the optimized experimental conditions, taking molecular weights and isoelectric points of given proteins (template protein: HTr; competitors: MYB and HSA) into consideration. As compared to the non-imprinted cryogels, the relative selectivity coefficients of these artificial antibodies for HTr/MYB and HTr/HSA were found to be 2.24 and 2.10 times higher, respectively.[32] In another study by Çetin and Denizli (2019), cryogels have been improved and novel HEMA-based micron-sized cryogels with equal size were synthesized in the presence of monomers that contain epoxy group and glycidyl methacrylate for HTr. In this study, micro-cryogels which can be synthesized in any size and shape were produced as immunoaffinity adsorbents for HTr adsorption from aqueous solutions. Immunoaffinity microcryogels were prepared by covalently immobilizing anti-HTr antibodies onto microcryogels through the epoxy groups of the microcryogels.[33]

In this study, we aimed to recognition of HTr from a different point of view, due to difficulties such as the inability to detect the amounts below the detection limit of the devices, the interference of proteins with each other, or the inability to desorption with full performance, etc. In the present study, HTr surface-imprinted particles were synthesized and embedded into cryogels to improve affinity properties by improving the surface area to deplete HTr from blood serum. In this study, HTr imprinted composite cryogel (HTr-MIPCC) was applied to fast protein liquid chromatography (FPLC) to separate HTr from both aqueous HTr solutions in the presence of other proteins and human serum samples.

## Experimental

### Materials

Sigma (St. Louis, MO, USA) was the supplier for 2-hydroxyethyl methacrylate (HEMA) and Poly (ethylene glycol) diacrylate (PEGDA); and BioRad (Hercules, CA, USA) for N, N, N', N'-Tetramethyl ethylenediamine (TEMED) and Ammonium persulfate (APS) to be used in the synthesis of the cryogel discs. HTr-MIP particles were synthesized using Glycidyl methacrylate (GMA) and Ethylene glycol dimethylacrylate (EGDMA) (Fluka A.G., Buchs, Switzerland). HTr and human serum albumin, and equine skeletal muscle myoglobin all with the purity of 98–100% (Sigma; St. Louis, MO, USA). Human plasma (Cat No: P4639) was purchased from Sigma (St. Louis, MO, USA). Other reagent-grade chemicals were supplied from Merck AG (Darmstadt, Germany). Barnstead (Dubuque, IA) ROpure LP® reverse osmosis unit was used to obtain ultra-pure water to be used in most of the steps of the study. Pre-filtration of buffer and samples were carried out using a 0.2-μm disc (Sartorius, Gottingen, Germany).

### Preparation of HTr-MIPCC

Synthesis of HTr-imprinted particles was carried out using GMA as a monomer in the presence of EGDMA as cross-linker, via suspension polymerization method, which was reported in a previous study[34]: 10 μmol of HTr was poured into the polymer suspension and stirred for 30 minutes in order to achieve proper monomer–template interaction. Polymerization was carried out at

40°C for 24 hours in the presence of HTr. The same procedure was performed without the addition of HTr for the synthesis of the non-imprinted (NIP) particles. The synthesized HTr-imprinted particles with the size range of 1–10 μm, were then embedded into Poly (2-hydroxyethyl methacrylate) (PHEMA) based cryogel plate (150×150 mm, thickness 0.5 mm). Briefly, polymer solution with 10% monomer concentration was prepared with HEMA and PEGDA (6:1 molar ratio) in 15 mL ultrapure water. HTr surface-imprinted particles were inserted into the polymer solution (200 mg particles/mL monomer), and degassing procedure with vacuum was applied for 10 minutes to remove water-soluble oxygen from the obtained polymer solution. APS and TEMED were added in the amount of 1% of the total amount of monomers in order to initiate polymerization providing proper conditions (at 0°C). After pouring the total polymer solution between two glass plates (spacer thickness: 0.5 mm), obtained system was left to freeze under suitable cryogelation conditions (16 for 24 hours). The final composite cryogel plate was left for thawing at 25°C and cut in disc shape (diameter: 1.6 mm). For the synthesis of NIP composite discs, the same procedure was performed adding non-imprinted particles instead.

The template removal procedure was carried out in a batch system with acetic acid and sodium dodecyl sulfate (SDS) mixture with the ratio of 10% v/v: 10% w/v, respectively. This process was continued until a certainty that no HTr remained in the cryogel structure so that all HTr-specific cavities are available. A spectrophotometer (UV–1601, Shimadzu, Japan) was used to control the removal of HTr from composite cryogel discs by measuring the absorbance value at 280 nm.

## Characterization studies

In order to investigate the gelation yield of the material, water content was removed from one of the swollen discs using oven (60°C). The amount of the water-free sample was measured ($m_{dried}$). The gel fractionation yield was determined using the following Equation (1):

$$Gelation\ yield\,\% = (m_{dried}/m_t) \times 100 \qquad (1)$$

where $m_{dried}$ is the weight of the dried disc and $m_t$ is the total amount of the monomers in the polymer solution. For the determination of the entire volume of macropores in the interior structure swollen disc, swollen disc was squeezed for the removal of water from the supermacropores of spongy cryogel disc sample (initial and final weight of the disc: $m_{swollen}$ and $m_{squeezed}$, respectively) and macroporosity was approximately calculated using the following Equation (2)

$$Macroporosity\,\% = (m_{swollen} - m_{squeezed})/m_{swollen} \times 100 \qquad (2)$$

Brunauer–Emmett–Teller (BET) analysis (Flowsorb II 2300, Micrometrics Instrument Corporation, Norcross, GA) that utilizes multipoint method was used for the determination of the specific surface area of the disc. SEM (JEOL JSM 5600, Jeol Co., Tokyo, Japan) analysis has been utilized to investigate the surface structure of the discs. Fourier transform infrared spectroscopy (FTIR) spectra of the discs were examined via FTIR Spectrometer (Nicolet iS10, Thermo Fisher Scientific, USA) between 4000 and 600 $cm^{-1}$.

## HTr adsorption studies from aqueous HTr solution

All adsorption studies of HTr-MIPCC from aqueous solution were examined in a batch system. For this purpose, the HTr-MIP composite was cut in cryogel disc form (0.5 mm x 1.6 mm). 20 HTr-MIPCC discs were equilibrated in 10 mM pH 5.0 acetate buffer for 30 minutes after washing with water. Adsorption studies such as pH, initial concentration, adsorption time, temperature, and the effect of ionic intensity were carried out to investigate the effectiveness of HTr adsorbed to HTr-MIPCC discs. In this context, the effect of the adsorption time in the range of 0–120 min, the effect of the temperature in the range of −4°C and +40°C; the effect of pH in the range of 4.0–7.0 of the aqueous solution to the adsorption capacity; the effect of ionic intensity in the range 0–0.1 M NaCl environment was performed. In addition, the effect of HTr desorption on reproducible adsorption was also investigated. For this purpose, HTr adsorbed HTr-MIPCC discs were desorbed with SDS and acetic acid (10% w/v, 10% v/v) solution. For repeatability studies, the adsorption-desorption cycle was repeated at least 10 times using the same HTr-MIPCC. The amount of HTr adsorption and desorption for the HTr-MIPCC was measured using the Bradford method using the equivalence HTr concentrations of the solutions before and after treatment with the HTr-MIPCC/NIPCC discs. The adsorption capacity (Q) was calculated using the following Equation (3):

$$Q = \left(C_o - C_f\right) \times V/m \qquad (3)$$

by measuring the solution (595 nm). Here, $C_o$ and $C_f$ represent the initial and final HTr concentration (mg/mL), V solution volume (mL), and m the total cryogel dry weight (g) used, respectively.

### FPLC separation studies

The separation of HTr in binary competitive protein solutions and human plasma was implemented in AKTA-FPLC (Amersham Bioscience, Uppsala, Sweden) system equipped to monitor and INV-907 injection valve. In order to apply samples to the FPLC, 20 pieces of template-free MIPCC discs were packaged into a GE Healthcare column (model: XK 26/40) shown as in Fig. 1.

The selectivity studies from aqueous protein solutions were performed, for this application, the binary protein mixtures were prepared with the competitors, HSA (Mw: 67.0 kDa, pI: 4.9) and IgG (Mw: 120.0 kDa, pI: 6.8–7.2), in the presence of template protein HTr (Mw: 80.0 kDa, pI: 5.2). The selective HTr adsorption studies from human serum were also performed, for this purpose, the commercially obtained human plasma samples were diluted in 1/10, 1/20, and 1/30-fold with 10 mM PBS buffer (pH 7.4). MIP and NIP-packed disc cryogels were carried out in GE Healthcare (model: XK 26/40) columns. 100 µL of injection volume of sample in PBS buffer (10 mM, pH 7.4) was applied. FPLC mobile phases A (10 mM phosphate buffered saline (PBS) buffer, pH 7.4) and B (10 mM PBS buffer in 2 M NaCl) was used for the adsorption and eluting process. The chromatographic separation was performed using a linear gradient at 1.0 mL/min of flow rate. Pre-filtration of buffers and protein samples were carried out using the 0.2-µm disc. Changes in absorbance values were tested at 280 nm. Chromatographic peaks were analyzed to find out the maximum capacity amounts and the specificity of the matrix for given samples, by determining, chromatographic parameters; capacity factor ($k'$), separation factor α; theoretical plate number (N), and resolution factor (Rs).

The capacity factor is calculated using the following Equation (4):

$$k' = (tR - to)/to,\ \alpha = k2'/k'1 \tag{4}$$

In here tR and to; are the retention times of the protein and the void marker (KBr), respectively. $k'^2$ is the capacity factor for HTr and $k'^1$ is the capacity factor for competitive proteins.

The resolution (Rs) factor is calculated as follows (5):

$$Rs = 2(tR,2 - tR,1)/(w2 + w1) \tag{5}$$

where, tR,1 and tR, 2 are the retention times of two adjacent peaks, w1 and w2 are the widths of the two adjacent peaks at the baseline. The number of effective layer (N) was determined using the peak height at the corresponding peak height fraction (w0.5), calculated as follows (6):

$$N = 5.54(tR/w0.5) \times 2 \tag{6}$$

Using the FPLC system, MIPCC and NIPCC columns were studied at different flow rates in order to evaluate the back-pressure profiles. Different flow rates affect the retention times of the compounds, especially when working with viscous liquids such as blood and serum.[35] The column backpressure in the FPLC system was evaluated by working at profile, flow rates of 2.0, 3.0, 4.5 mL/min.

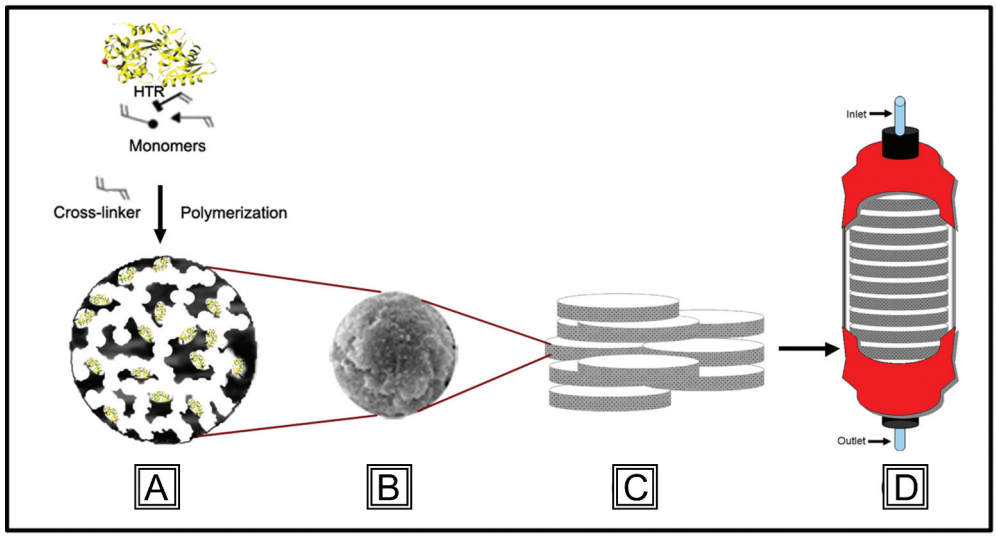


**Figure 1.** Preparation Scheme of MIPCC Discs. (A) Synthesis of HTr surface imprinted particles. (B) Characterization of particles. (C) Embedding particles into cryogel discs. (D) Packing cryogel discs into FPLC column for application.

## Results and discussion

### Characterization studies

Besides the advantages of cryogels, these spongy materials have deficits including reduced surface area and a further decrease in adsorption capacity.[36] The separation of biomolecules requires the advanced adsorption capacity of cryogels. In order to improve the surface area of the supermacroporous cryogels, thus increasing the adsorption capacity, inserting molecularly imprinted particles into cryogels has been considered to be an effective technique.[37] Particles embedded in cryogels are a particular form of monolithic column that uses the unique characteristics of cryogels and particles to increase the surface area. High loading capacity is achieved by using an adsorbent with a high pore size distribution. The adsorbent's large pores allow biomolecules to be transported without compromising their 3D structure.[38] SEM photos of HTr-MIP particles demonstrate the spherical structure of the particles with sizes between 1 and 10 μm and their porous structure encircled by a rigid surface, in the dry condition. This feature of the material is to be thought of as one of the reasons causing a significant increament in the surface area. Advances in the interior surface area of the particles eliminate the effect of diffusional resistance simplifying the mass transfer so that the adsorption capacity of the material will be even more elevated.

HTr-MIP particles (200 mg) were loaded into per mL of PHEMA cryogels. The addition of surface imprinted particles into the cryogel plate has resulted in an increased surface area, enhancing the capacity of composite cryogel for HTr adsorption up to 86% and gel fractionation yields reached up to 83% as compared to non-embedded cryogels. It can be concluded that the addition of the HTr-MIP particles has not any significant effect on the polymerization yield. Supermacroporous structure has been analyzed in the swollen state and the capacity of water uptake of the pores was determined as about 62% (Table 1). Supermacroporosity can be investigated within the scope of the flow rate of the sample through the cryogel. HTr-MIP particles in the structure of PHEMA cryogel have resulted in a reduction in the flow resistance of the gel matrix (at hydrostatic pressure, ca. 0.01 mPa) and the flow resistance was calculated as 55 cm/h (Table 1). BET analysis was performed for the determination of the specific surface areas of HTr-MIPCC discs, and it was found to be 232.0 $m^2$/g cryogel, about ten-fold larger than traditional non-composite cryogel (25.2 $m^2$/g) (Table 1).[34] In the study of Aydoğan et al. (2012), specific surface area of molecularly imprinted Poly (hydroxyethyl Methacrylate-N-methacryloyl-(L)-glutamic acid)-$Fe^{3+}$ was found to be 25.2 $m^2$/g, with gelation yield up to 95.3%. Relatively lower swelling ratio and macroporosity, as well as the higher linear flow resistance up to 116 cm/h were reported in this study, as compared to that of HTR-MIPCC and HTr-NIPCC.[40] In the study of Oktay Başeğmez et al. (2021), HEMA-based particles were found to have a specific surface area up to 45.43 $m^2$/g, with 87.4% swelling ratio.[17] In another study (Yıldırım and Baydemir Peşint, 2021), relatively better surface area has been reported for HEMA-based non-composite cryogel columns (52 $m^2$/g) as compared to other non-composite cryogels in literature.[44] In the study of Le Noir et al. (2007), composite monoliths were synthesized embedding macroporous gels with PVA-based

**Table 1.** Structural characteristics, flow dynamics, and swelling properties of HTr MIPCC, NIPCC and their comparison of literature.

| Cryogel Membrane | Surface Area ($m^2$/g) | Equilibrium Swelling Ratio (%) | Yield (%) | Linear Flow Resistance (cm/h) | Macroporosity (%) | Ref |
|---|---|---|---|---|---|---|
| HTr-MIPCC | 220 | 91 | 85 | 55 | 65 | Present work |
| HTr-NIPCC | 218 | 92 | 89 | 56 | 68 | Present work |
| Macroporous gels embedded with PVA-based molecularly imprinted polymers | 376 | N/A | N/A | N/A | 83.6 | [39] |
| Poly(hydroxyethyl methacrylate-N-methacryloyl-(L)-glutamic acid-Fe3+ – L-GLU | 25.2 | 10.3 | 95.3 | 116 | 62 | [40] |
| Acrylamide-based Lysozyme-imprinted cryogel | N/A | 24.5 ± 3 | 72 | N/A | N/A | [41] |
| poly(hydroxyethyl methacrylate-N-methacryloyl-(l)-histidine methyl ester) cryogel discs | 16.1 (±0.26) | 922 (±15) | N/A | N/A | 82.7 (±0.49) | [42] |
| Tyr-imprinted cryogel cartridge | 39.05 | 88.2 ± 0.02 | N/A | N/A | N/A | [43] |
| Hydroxyethyl methacrylate-based Angiotensin(II) imprinted cryogel columns | 52 | 94.3 | 88 | N/A | 82 | [44] |
| Hydroxyethyl methacrylate-based Neoptrein imprinted cryogel columns | 22 | 88 | 86 | N/A | 72 | [45] |
| 2-4-vinylphenylboronic acid containing 2-hydroxyethyl methacrylate cryogel membranes | 17.2 | 88.3 | 82.6 | N/A | 72 | [46] |
| Hydroxyethyl methacrylate-based ergosterol imprinted particles | 45.43 | 87.4 | 85 | N/A | N/A | [17] |
| poly(2-hydroxyethyl methacrylate-co-N-methacryloyl-(L)-tyrosine methyl ester) monolithic cryogel column | 27 | 84.5 | N/A | N/A | 63.1 | [22] |

*N/A: Not applicable

molecularly imprinted polymers and specific surface area was achieved up to 376 $m^2$/g polymer, with 83.6% macroporosity. Water flow path through the monolith column was determined as 580 cm/h and 100% of initial weight after drying was re-swollen within a few seconds and demonstrates the advantages of composite cryogels.[39] As a result of a comprehensive and comparative literature review, it has been demonstrated that composite cryogels are structurally more favorable than non-composite cryogels.

According to the FTIR spectra of MIPCC and NIPCC, it was concluded that both results have specific broad peak at about 3400 $cm^{-1}$, demonstrating the O-H stretching vibrations. Symmetric & asymmetric C-H stretching vibrations were appointed to the bands at around 2950 $cm^{-1}$ and 2883 $cm^{-1}$. The presence of C-O stretching vibrations was concluded due to the presence of the band of medium intensity at 1721 $cm^{-1}$. The medium O-H stretch peak based on the functional groups of the HEMA monomer was observed at 1420–1330 $cm^{-1}$ in the vibration spectrum of HTr-MIPCC and NIPCC. It was observed that Amide I and Amide II groups had characteristic tensile vibration bands around 1600 and 1500 $cm^{-1}$. The appearance of strong bands at 1650 $cm^{-1}$ (C = O, amide I), 1535 $cm^{-1}$ (N-H bending, amide II) indicates the incorporation of GMA monomer into the polymer structure. The medium peaks seen in the spectrum of MIPCC, different from the NIPCC spectrum seen at 1535 and 1651 cm-1, respectively, express the stretching of N-H and C-N stretch and C = O and C = N groups in the amine II group of imprinted cavities in MIPNs. These distinctive peaks might indicate MIPCC's desire to create more hydrophobic interactions than NIPCC (Fig. 2).[47–50]

Figures 3 and 4 show the SEM images of the interior structures of the HTr-MIP particles, NIP particles, and MIPCC discs. In Fig. 3, the HTr-MIP and NIP particles show a homogeneous distribution. It is seen that the particle surface roughness is increased at a larger magnitude (Fig. 3E). This is further evidence of increased surface area. It is also seen at 10.00 K X magnitude that the surfaces of NIP particles are more smooth. This could roughly be an indication that imprinting was successful. The MIP and NIP particles showed high monodispersity with a spherical shape, and their size was found around 1–10 μm. The flow of the mobile phase is maintained via an interconnected macroporous structure (10–100 μm in diameter). According to SEM images, HTr-MIP and NIP particles were homogeneously distributed in the structure of cryogel network. HTr molecules are much smaller than pore dimensions so that these molecules can easily pass through the pores and find their specific cavities. Flow resistance can be thought of as insignificant in practice, owing to the convective flow through the interconnected porous structure. The elasticity and sponge-like structure of HTr-MIPCC discs make it possible to squeeze them by hand to remove the water inside the macropores. Because of the shape memory of the cryogels, when the squeezed cryogel disc was thrown into the water, it absorbed the water and restored to its initial size and shape in a few seconds.

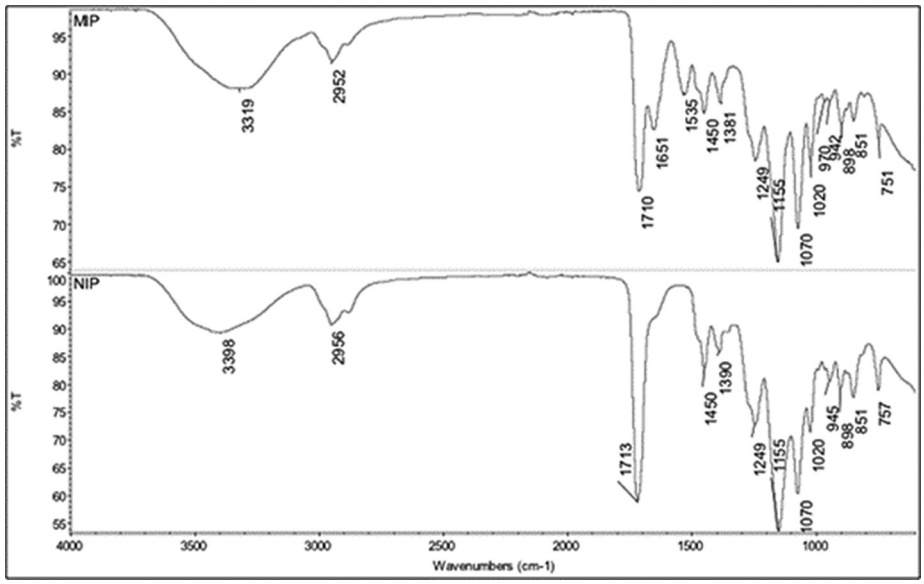


**Figure 2.** FTIR spectra of HTr-MIPCC and NIPCC.

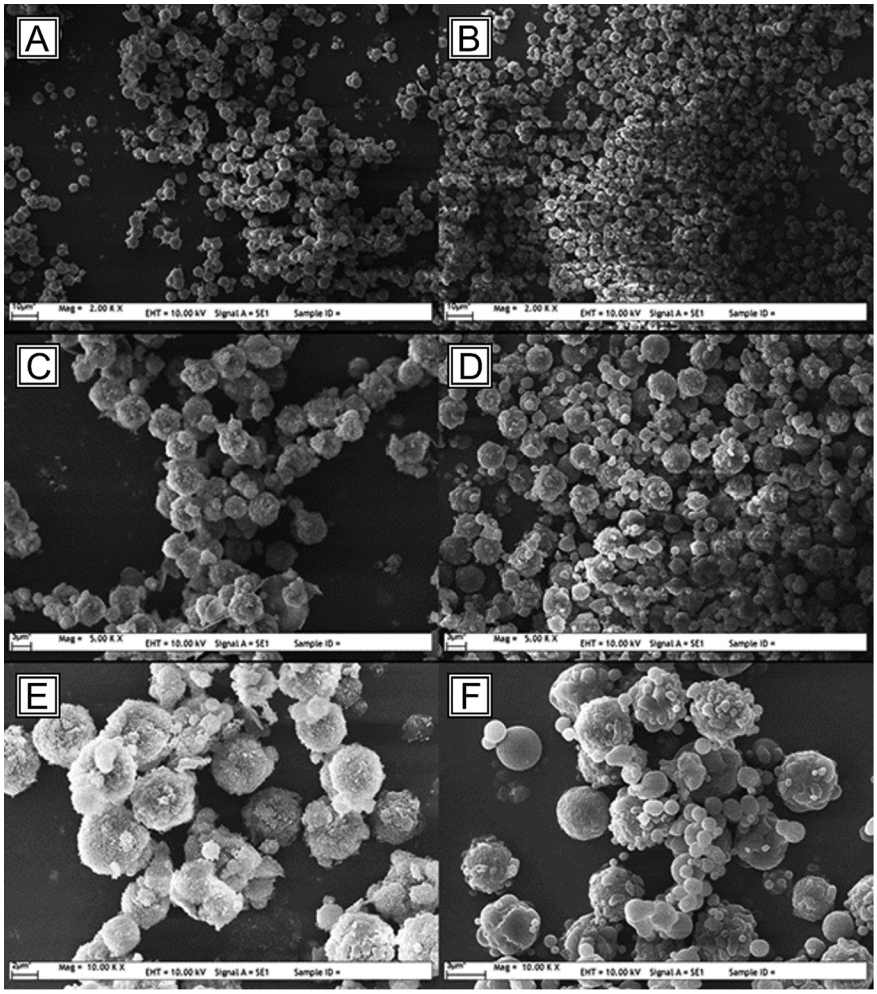


**Figure 3.** HTr surface-imprinted particles with 2.00 K X (A), 5.00 K X (C) and 10.00 K X (E) magnification and non-imprinted particles with 2.00 K X (B), 5.00 K X (D) and 10.00 K X (F) magnification.

### *HTr adsorption studies from aqueous HTr solution*

The last step of HTr-MIPCC synthesis is the effective removal of HTr from the composite cryogel so that the adsorption efficiency can be examined. As a result of removing the target HTr molecules from the cryogel, chemically and topologically selective cavities are obtained for the HTr, which is imprinted in the polymeric structure and in a mixture, the template molecule (HTr) can be selectively adsorbed on the polymeric structure. In order to effectively remove HTr from the composite cryogel structure, 1% SDS-Tris base solution was used. Because of its amphipathic properties, SDS is commonly utilized in desorption processes. It enters the embedded locations by binding to the protein chain with its hydrocarbon tail. Surfactant molecules, on the other hand, surround the protein chain and denature it. The fact that SDS has a pole group adds to the benefits of using it as a denaturant.[51] It was recorded that the template molecule (HTr) was removed by 85% as a result of repeated washing processes.

Adsorption studies for the HTr reconnection efficiency from the aqueous solution were examined in the batch system. In order to examine the effect of pH on adsorption capacity, the pH of the aqueous solution was changed between 4.0 and 7.0, and the maximum adsorption capacity was observed at pH 5.2 (Fig. 5A). The reason for this is that the isoelectric point of HTr is at this pH and shows maximum back adsorption efficiency in the most suitable geometric structure. HTr adsorption over time was shown in Fig. 5B. Adsorption is very fast at the beginning but as expected, the adsorption capacity reached the plateau in the first 60 minutes due to the filling of unique molecularly imprinted cavities to which HTr can be adsorbed on the composite cryogel surface. At this time, the maximum adsorption amount for HTr is 2.86 mg/g dry MIPCC. Specific molecular cavities for

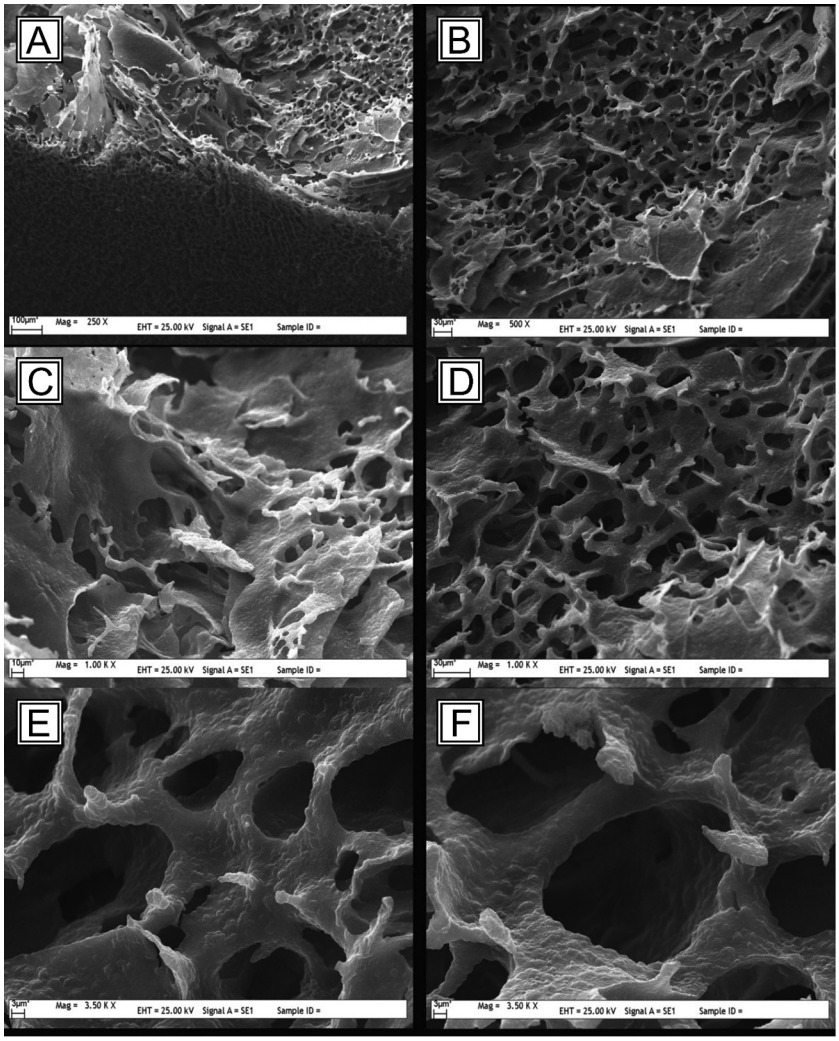


**Figure 4.** Composite cryogels with different magnification levels. SEM photographs of HTr-MIPCC discs with 250X (A), 500X (B), 1.00 K X (C and D) and 3.50 K X (E and F) magnification.

HTr are formed in the HTr-MIPCC structure by imprinting. These cavities in the HTr-MIPCC discs have a geometric and chemical affinity for HTr in the solution and have high adsorption properties. The effect of temperatures on HTr adsorption on HTr-MIPCC discs was also summarized in Fig. 5C. In the study performed, the maximum adsorption amount was obtained at the temperature of 40°C. For HTr-MIPCC, this value is 3.02 mg/g dry HTr-MIPCC. Increasing temperature also increases the interaction between HTr and adsorbent, thereby increasing HTr adsorption. The effect of ionic strength was testing by changing NaCl concentration on HTr adsorption is given in Fig. 5D. As seen in the figure, with the NaCl concentration reaching up to 0.75 M, HTr adsorption increased, and at higher salt concentrations, the adsorption capacity of the HTr-MIPCC decreased. Adding salt to the adsorption medium causes increased hydrophobic interactions in proteins. This shows that increasing salt concentration up to a certain rate contributes to hydrophobic interactions, thus increasing HTr-adsorbent interaction. After the 0.75 M NaCl concentration, salt molecules reduce the HTr solubility by holding the water in the environment. It also reduces ionic interactions, preventing HTr from adsorption to MIPCC. These results show us that ionic interactions, as well as hydrophobic interactions, have an important role in MIPCC adsorption of HTr.[52]

The change of HTr adsorption to HTr-MIPCC discs with the initial equilibrium concentration of HTr in the medium and the Langmuir and Freundlich adsorption isotherms shown in Fig. 6A. As seen from the figure, with the increase of HTr initial concentration in the solution, the amount of HTr adsorbed per unit HTr-MIPCC discs increased rapidly up to 0.5 mg/mL initial HTr. The plateau was reached at the concentration value (10.96 mg/g dry cryogel). The concentration difference ($\Delta C$), which is the driving force for adsorption, increases with increasing concentration. An increase in

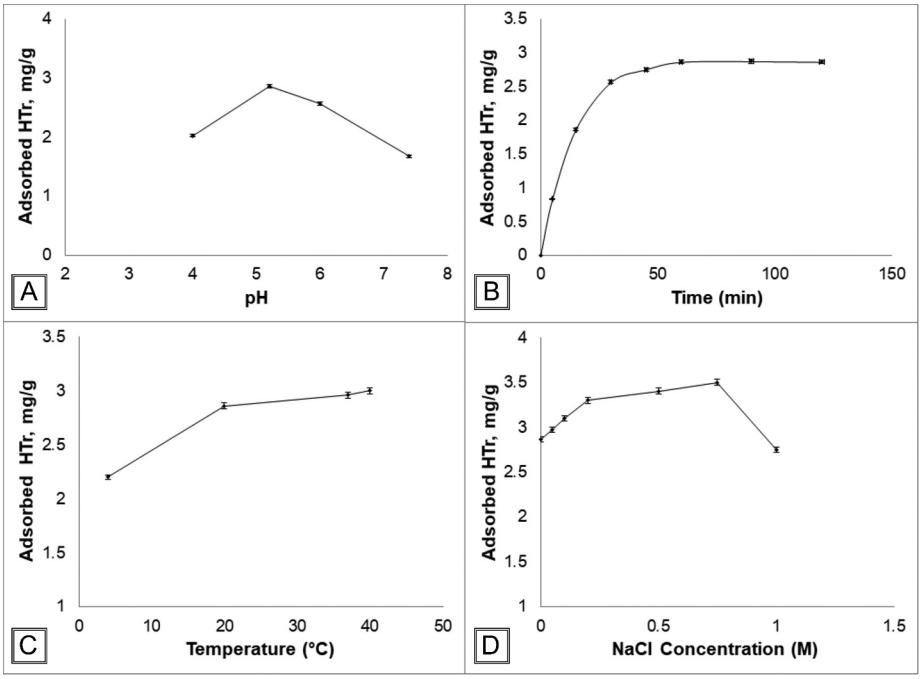


**Figure 5.** The effect of (A) pH, (B) time, (C) temperature, (D) ionic strength on HTr adsorption onto HTr-MIPCC. Experimental conditions: HTr equilibrium concentration: 0.1 mg/mL, $V_{total}$: 10 mL, $m_{cryogel}$: 260 mg, T: 20°C, pH: 5.2.

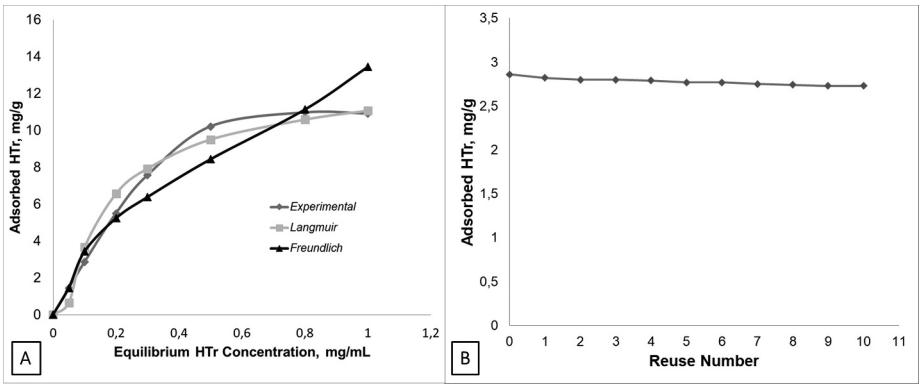


**Figure 6.** (A) Effect of equilibrium initial HTr concentration HTr adsorption and Langmuir and Freundlich adsorption models. Experimental conditions: pH solution: 5.2, $V_{total}$: 10 mL, $m_{cryogel}$: 260 mg, t: 60 min, T: 20°C. (B) Reusability of HTr-MIPCC. Experimental conditions: pH solution: 5.2, HTr initial concentration: 0.1 mg/mL, $V_{total}$: 10 mL, cryogel: 260 mg, t: 60 min.

**Table 2.** Langmuir and Freundlich adsorption isotherm constants for HTr adsorption.

| | Experimental | Langmuir Constants | | | Freundlich Constants | | |
|---|---|---|---|---|---|---|---|
| | $Q_{ex}$ (mg/g) | $Q_L$ (mg/g) | b (ml/mg) | $R^2$ | $Q_F$ (mg/g) | n | $R^2$ |
| MIPCC | 10.96 | 12.03 | 15.39 | 0.9913 | 15.21 | 2.39 | 0.9597 |

adsorption capacity is also observed with increasing driver force. When this experiment was performed for NIPCC discs, the maximum adsorption capacity was obtained as 5.89 mg/g NIPCC. The adsorption behavior of HTr was also investigated using obtained data according to Langmuir and Freundlich adsorption models. Langmuir adsorption model defines monolayer adsorption and can be calculated as follows (7)

$$Ceq/Q = 1/(Qmax.\,b) + (Ceq/Qmax) \quad (7)$$

Q is the actual HTr adsorption capacity (mg/g), Ce is the equilibrium HTr concentration (mg/mL), and b is the Langmuir adsorption constant (mL/mg). Whereas the Freundlich describes the multilayer adsorption models and calculated using the following Equation (8):

$$ln\,Qeq = ln\,Q_f + (1/n \times ln\,Ceq) \quad (8)$$

Here, $Q_F$ is the Freundlich adsorption constant, Ce is the equilibrium HTr concentration (mg/mL), and n is the Freundlich exponent.[53] As can be seen clearly in Fig. 6A, the Langmuir adsorption plots are well fitted with experimental adsorption plots than Freundlich. Correlation coefficients comparisons are given in Table 2; it was clear that the correlation coefficient for Langmuir isotherm ($R^2$ = 0.99) was higher than that for Freundlich isotherm ($R^2$ = 0.95). When comparing the Q values, it can be seen that the Langmuir $Q_L$ (12.03 mg/g) is close to the experimental $Q_{ex}$ (10.96 mg/g) value than Freundlich $Q_f$ (15.21 mg/g).

Fig. 6B shows the reusability of HTr-MIPCC. For each cycle, HTr-MIPCC discs were desorbed with SDS and acetic acid (10% w/v: 10% v/v) solution after each adsorption. For repeatability studies, the adsorption-desorption cycle was repeated at least 10 times using the same HTr-MIPCC, the desorption rate was recorded as 95% and the adsorption capacity was decreased only 5%, this can be negligible and it can be said that newly synthesized HTr-MIPCC are reusable adsorbents.

## FPLC separation studies

The efficacy of HTr-MIPCC discs column in HTr separation was determined using albumin and IgG proteins. The selectivity studies from aqueous protein solutions were performed, for this application, the binary protein mixtures were prepared with the competitors, HSA and IgG, in the presence of template protein HTr. The chromatograms obtained for the HTr-MIPCC and NIPCC disc columns were compared with each other in Fig. 7A and B respectively. As shown in Fig. 7A, at t = 17 min, the adsorbed HTr was separated accurately from the column. In the HTr elution step, using NaCl solution as a desorption agent enhances the amount of HTr removed from MIPCC. The repulsive electrostatic interactions between the MIPCC and HTr molecules were attributed for this.[54] However, the other proteins under comparison gave approximately the same chromatogram profile for the HTr-MIPCC and NIP composite cryogel disc (Fig. 7B). This demonstrates that albumin and IgG leave the column without adherence, in other words, these proteins do not interact with the HTr-MIPCC disc sufficiently. These results confirm that the HTr-MIPCC column has only HTr-specific molecular memory and selectively recognizes HTr.

Table 3 shows the capacity factor (k') and separation factor (α) values for HTr-MIPCC and NIPCC disc columns calculated using the retention times of the competitive proteins (HIgG and HSA), and target molecule (HTr). According to this table, the k' value of HTr-MIPCC column for HTr is greater than the k' value of the NIP for the HTr. The k' values calculated for the NIP composite column indicate that this column interacts with all proteins. At the same time, the k' value of the MIP column for the HTr is greater than that of the NIP column. This clearly shows that the HTr-MIPCC disc column has HTr-specific recognition sites. Furthermore, the α value calculated for the HTr-MIPCC disc column is greater than the values calculated for the NIPCC, indicating that the separation factor of the HTr-MIPCC is better than that of the NIPCC.

The imprinting factor (IF) is calculated to determine the specific and nonspecific interactions of the target molecule (HTr) with the HTr-MIPCC and NIPCC (Table 4). The IF values calculated for HTr are greater than 1, indicating that there are specific interactions between HTr and HTr-MIPCC, even in the presence of competitive proteins. The selectivity factor (SF) is calculated to assess whether the adsorption behavior of HTr-MIPCC for HTr is selective. According to the results obtained from the chromatograms in Fig. 7A and B, the SF value for HTr-MIPCC discs was calculated to be greater than 1. In chromatographic studies performed with HTr-MIPCC disc column, HTr molecule exhibits much more selective adsorption behavior for HTr-MIPCC than NIPCC.

## Separation of HTr from human plasma

HTr-MIPCC disc column was used to investigate the separation of HTr from human plasma diluted with 1/10, 1/20, and 1/30 dilution rates. Fig. 8 shows a chromatogram for the separation of HTr from human plasma with the HTr-MIPCC disc column. Bound HTr (bound fraction) and unbound plasma proteins (unbound fraction) are shown in the chromatogram. As can be seen from the chromatogram in Fig. 8, the other plasma proteins were separated from the column without adsorption at t = 1.4 min, while the HTr was retained in the column until the 15$^{th}$ minute, then separated from the column at the 17$^{th}$ minute by the action of mobile phase B. It is known that there is a proportionality between the capacity factor and the number of effective layer (N). The MIP column's capacity factor (k') value for the HTr is higher than the NIP

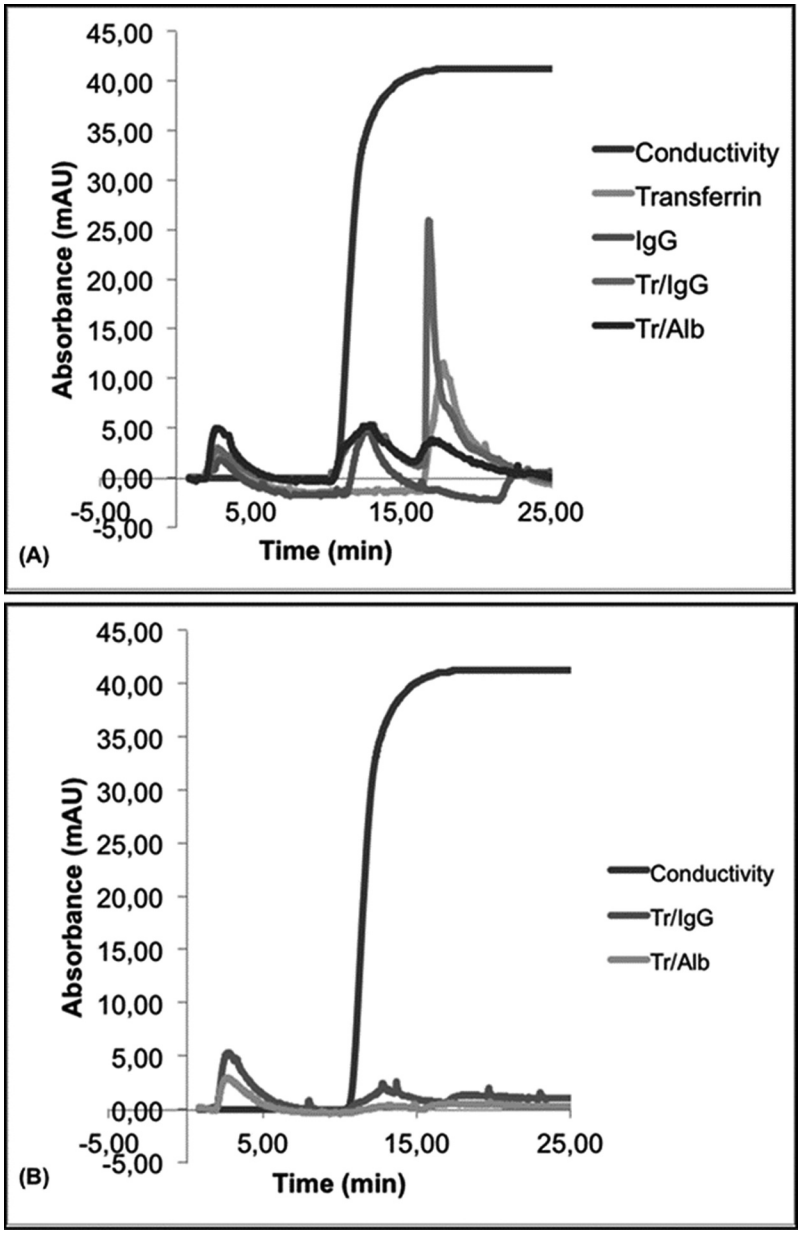


**Fig. 7 Aand B** Separation of HTr, Alb and IgG proteins in (A) HTr-MIPCC (B) NIPCC disc column. Protein concentration: 0.1 mg/mL; sample volume: 100 µL; mobile phase A: 10 mM PBS, pH 7.4; mobile phase B: 10 mM PBS, 2 M NaCl; flow rate: 1 mL/min, back pressure: 0.56 MPa; λ: 280 nm.

**Table 3.** k′ and α values of HTr-MIPCC and NIPCC disc columns.

| Polymer | | Unbound Protein (min) | Bound Protein (min) | Bound HTr (min) | Capacity Factor (Protein) $k' = (t\text{-}t_o)/t_o$ | Capacity Factor (HTr) $k' = (t\text{-}t_o)/t_o$ | Separation Factor (α) $\alpha = k'_{HTr}/k'_{protein}$ |
|---|---|---|---|---|---|---|---|
| **HTr-MIPCC** | HTr/HSA | 2.68 | 12.38 | 17.64 | 44.85 | 64.33 | 1.43 |
| | HTr/HIgG | 2.52 | 12.15 | 17.13 | 44.00 | 62.44 | 1.41 |
| **NIPCC** | HTr/HSA | 2.28 | 12.76 | 17.00 | 46.26 | 61.96 | 1.33 |
| | HTr/HIgG | 2.57 | 12.73 | 16.92 | 46.15 | 61.66 | 1.33 |

**Table 4.** IF and SF values of HTr-MIPCC and NIPCC disc column.

| | Protein | HTr | |
|---|---|---|---|
| | Imprinting Factor (IF) | Imprinting Factor (IF) | Selectivity Factor (SF) |
| | $IF = k'_{MIP}/k'_{NIP}$ | $IF = k'_{MIP}/k'_{NIP}$ | $SF = IF_{HTr}/IF_{protein}$ |
| **HTr/HSA** | 0.969 | 1.038 | 1.071 |
| **HTr/ HIgG** | 0.953 | 1.012 | 1.062 |

column's. This definitely demonstrates the presence of HTr-specific recognition sites in the HTr-MIPCC disc column. In moreover, the separation factor (α) value produced for the HTr-MIPCC disc column is higher than the values calculated for the NIPCC, showing that the HTr-MIPCC has a better separation factor than the NIPCC. HTr-MIPCC disc column shows high selectivity to HTr with specific binding sites formed during molecular imprinting.[55]

Table 5 shows the retention time ($t_R$), capacity factor (k'), separation factor (α), separation value (Rs), and the number of effective layer (N) of the HTr-MIPCC disc column for HTr and other plasma proteins. According to the results, it can be seen that $t_R$ and therefore k' values of HTr are much higher than other proteins, as well as the α values of HTr. These results demonstrate that the interaction between HTr and HTr-MIPCC disc column is quite well. In a chromatographic system, Rs value greater than 1.0 shows that the separation of the two proteins is effective.[37] Table 5 shows that Rs values for plasma proteins are greater than 1.0. According to the results, HTr-MIPCC disc column is effective in separation of dual-protein solutions. The number of effective layer (N) values indicates that the physical properties of the HTr-MIPCC disc column are suitable for the separation of HTr.

**Table 5.** Chromatographic separation data of HTr-MIPCC disc column.

| Component | tR | N | CF | α | Rs |
|---|---|---|---|---|---|
| Plasma proteins (Unbound fraction) | 1.41 | 57 | 4.42 | - | - |
| HTr (Bound fraction) | 17.26 | 7361 | 65.38 | 14.78 | 29.83 |

## FPLC back pressure profile

In FPLC applications, it is desired that the pressure required to pass the liquid through any column is as low as possible. In this case, the entire mobile phase must be able to pass through the prepared cryogel column. This is related to the liquid permeability of the cryogel, which depends entirely on the pore size. Application of very high pressure can damage a cryogel with the same pore size as the pores in typical macroporous microspheres. Cryogels, which have a large number of interconnected macroporous structures, have low flow resistance. It is also desirable to have a large surface area to achieve high separation capacity. High surface area is generally a property of materials with smaller pore structure. Therefore, there should be a balance between low flow resistance and high surface

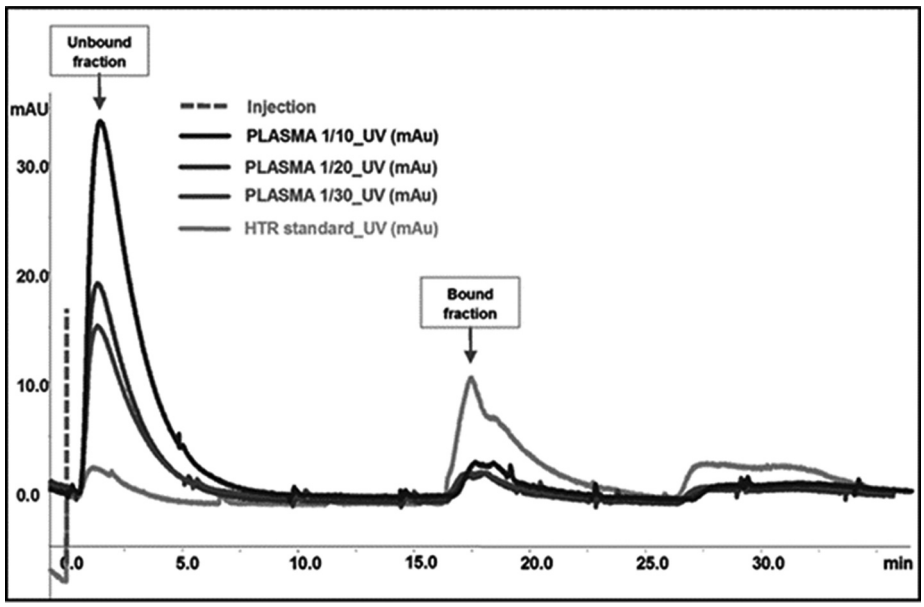


**Figure 8.** HTr separation from human plasma with HTr-MIPCC disc column. Plasma concentration: 1/10, 1/20, 1/30 dilution ratio; sample volume: 100 µL; mobile phase A: 10 mM PBS, pH 7.4; mobile phase B: 10 mM PBS, 2 M NaCl; flow rate: 1 mL/min, back pressure: 0.56 MPa; λ: 280 nm.

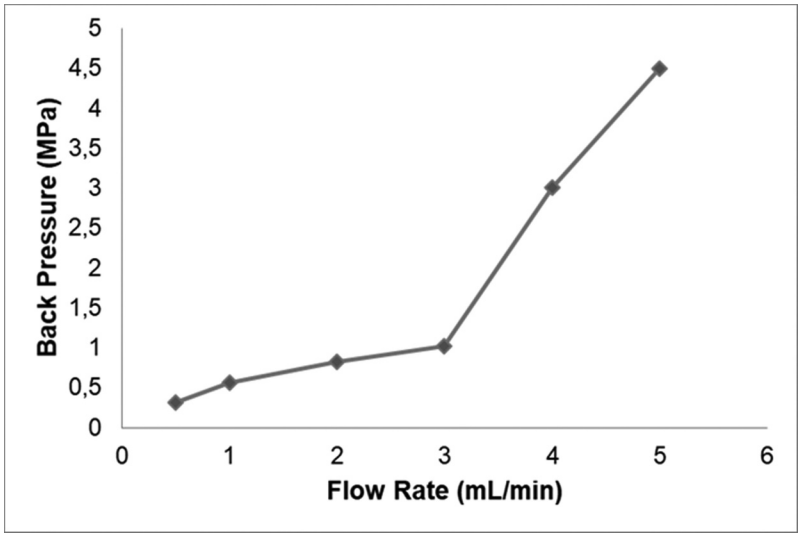


**Figure 9.** Effect of flow rate on back pressure for HTr-MIPCC disc column.

area. An ideal cryogel should contain large pores for reduced flow resistance and small pores to form an interconnected porous structure for high separation capacity. Fig. 9 shows the back-pressure profile of the synthesized HTr-MIPCC disc column. As can be seen from the figure, HTr-MIPCC disc column shows low flow resistance at flow rates of 0.5–3 mL/min and works ideally. Above this value, a sudden backpressure increase is observed.

## Conclusion

In this study, HTr surface imprinted particles modified cryogel discs (HTr-MIPCC) were synthesized firstly and applied for HTr separation from human serum in a single step. The FPLC system was used for HTr separation from both binary protein solutions of HTr and human serum successfully. Obtained results showed that the HTr-MIPCC discs are suitable columns for HTr separation from human serum and this method can be used for designing new MIP adsorbents with high selectivity. According to the results of this study, it was concluded that these novel composite cryogels are excellent alternatives of affinity matrixes for the detection and selective depletion of HTr directly from blood serum. The HTr-MIP particles were successfully prepared with a spherical shape and monosize form, according to FTIR and SEM characterizations. Variations in pH, starting HTr concentration, and adsorption time were used to find the best adsorption conditions of HTr-MIPCC. The addition of surface imprinted particles into the cryogel disc has resulted in an increased surface area, enhancing the capacity of composite cryogel for HTr adsorption up to 10.96 mg/g and gel fractionation yields reached up to 83%. The addition of surface imprinted particles into the cryogel plate has resulted in an increased surface area, enhancing the capacity of composite cryogel for HTr adsorption up to 86%. The HTr-MIPCC discs were packaged into a Fast Protein Liquid Chromatography (FPLC) column for selective depletion of HTr from human serum. It was calculated that the HTr-MIPCC is 1.071 and 1.062 times selective for HTr than HSA and HIgG, respectively. In conclusion, MIPCC with distinctive structure and increased adsorption capacity and specificity for HTr can be used in proteome studies.

## Highlights

- Human Transferrin (HTr) imprinted composite cryogel disks (HTr-MIPCC) were produced
- Distinctive structure and increased adsorption capacity were obtained
- HTr adsorption onto HTr-MIPCC disks up to 10.96 mg/g was achieved
- HTr-MIPCC was found to be 1.071 and 1.062 times selective for HTr than competitors
- HTr-MIPCC was examined in terms of selective depletion of HTr from human serum

## Acknowledgements

This project was financially supported by The Scientific and Technological Research Council of Turkey (TUBITAK) within the scope of 3001-Initial R&D Projects Support Program [project number 114Z664].

## Disclosure statement

The author(s) declare that they have no competing interests or personal relationships with other people or organizations that could have appeared to affect the study reported in this paper.

## Funding

This project was financially supported by The Scientific and Technological Research Council of Turkey (TUBITAK) within the scope of 3001-Initial R&D Projects Support Program [project number 114Z664].

## Author contributions

Gülgün Aylaz and Okan Zenger performed the research equally. Gözde Baydemir Peşint and Müge Andaç designed and wrote the paper.

[1] Steere, A. N.; Byrne, S. L.; Chasteen, N. D.; Mason, A. B. Kinetics of Iron Release from Transferrin Bound to the Transferrin Receptor at Endosomal pH. *Biochim. Biophys. Acta Gen. Subj.* 2012, 1820(3), 326–333. DOI: 10.1016/j.bbagen.2011.06.003.

[2] Muckenthaler, M. U.; Rivella, S.; Hentze, M. W.; Galy, B. A Red Carpet for Iron Metabolism. *Cell*. 2017, 176, 139–148. https://doi.org/10.1016/j.cell.2016.12.034.

[3] Murakami, Y.; Saito, K.; Ito, H.; Hashimoto, Y. Transferrin Isoforms in Cerebrospinal Fluid and Their Relation to Neurological Diseases. *Proc. Japan Acad. Ser. B Phys. Biol. Sci.* 2019, 95(5), 198–210. DOI: 10.2183/pjab.95.015.

[4] Anderson, G. J.; Frazer, D. M. Current Understanding of Iron Homeostasis. *Am. J. Clin. Nutr.* 2017, 106(Supplement 6), 1559S–1566S. DOI: 10.3945/ajcn.117.155804.

[5] Tandara, L.; Salamunic, I. Iron Metabolism: Current Facts and Future Directions. *Biochem. Medica.* 2012, 22, 311–328. DOI: 10.11613/BM.2012.034.

[6] Grant, B. D.; Donaldson, J. G. Pathways and Mechanisms of Endocytic Recycling. *Nat. Rev. Mol. Cell Biol.* 2009, 10(9), 597–608. DOI: 10.1038/nrm2755.

[7] Cornelissen, A.; Guo, L.; Sakamoto, A.; Virmani, R.; Finn, A. V. New Insights into the Role of Iron in Inflammation and Atherosclerosis. *EBioMedicine*. 2019, 47, 598–606. DOI: 10.1016/j.ebiom.2019.08.014.

[8] Ogun, A. S.; Adeyinka, A. Biochemistry, Transferrin, StatPearls - NCBI Bookshelf; 2021: 1–4. https://www.ncbi.nlm.nih.gov/books/NBK532928/ .

[9] Schalich, K. M.; Herren, A. W.; Selvaraj, V. Analysis of Differential Strategies to Enhance Detection of Low-abundance Proteins in the Bovine Serum Proteome. *Anim. Sci. J.* 2020, 91(1), 1–14. DOI: 10.1111/asj.13388.

[10] Polaskova, V.; Kapur, A.; Khan, A.; Molloy, M. P.; Baker, M. S. High-abundance Protein Depletion: Comparison of Methods for Human Plasma Biomarker Discovery. *Electrophoresis*. 2010, 31(3), 471–482. DOI: 10.1002/elps.200900286.

[11] Ohshiro, K.; Rosenthal, D. I.; Koomen, J. M.; Streckfus, C. F.; Chambers, M.; Kobayashi, R.; El-Naggar, A. K. Pre-analytic Saliva Processing Affect Proteomic Results and Biomarker Screening of Head and Neck Squamous Carcinomta. *Int. J. Oncol.* 2007, 30, 743–749. DOI: 10.3892/ijo.30.3.743.

[12] Baydemir, G.; Odabasi, M. A Novel Chromatographic Media: Histidine-Containing Composite Cryogels for HIgG Separation from Human Serum. *Affin. Chromatogr. Methods Protoc. Methods Mol. Biol.* 2015, 209–217. DOI: 10.1007/978-1-4939-2447-9_18.

[13] Okay, O. Polymeric Cryogels Macroporous Gels with Remarkable Properties; 2014. DOI: 10.1007/978-3-319-05846-7.

[14] Pan, J.; Chen, W.; Ma, Y.; Pan, G. Molecularly Imprinted Polymers as Receptor Mimics for Selective Cell Recognition. *Chem. Soc. Rev.* 2018, 47(15), 5574–5587. DOI: 10.1039/c7cs00854f.

[15] Gao, M.; Gao, Y.; Chen, G.; Huang, X.; Xu, X.; Lv, J.; Wang, J.; Xu, D.; Liu, G. Recent Advances and Future Trends in the Detection of Contaminants by Molecularly Imprinted Polymers in Food Samples. *Front. Chem.* 2020, 8, 1–20. DOI: 10.3389/fchem.2020.616326.

[16] Aylaz, G.; Kuhn, J.; Lau, E. C. H. T.; Yeung, C. C.; Roy, V. A. L.; Duman, M.; Yiu, H. H. P. Recent Developments on Magnetic Molecular Imprinted Polymers (Mmips) for Sensing, Capturing, and Monitoring Pharmaceutical and Agricultural Pollutants. *J. Chem. Technol. Biotechnol.* 2021, 96(5), 1151–1160. DOI: 10.1002/jctb.6681.

[17] Oktay Başeğmez, H. İ.; Baydemir Peşint, G.; Nergiz, M.; Zenger, O. Determination of Mold Contamination Using Ergosterol Imprinted Particles. *Biotechnol. Prog.* 2021, 37(1), 1–7. DOI: 10.1002/btpr.3089.

[18] Belbruno, J. J. Molecularly Imprinted Polymers. *Chem. Rev.* 2019, 119(1), 94–119. DOI: 10.1021/acs.chemrev.8b00171.

[19] Ahmad, O. S.; Bedwell, T. S.; Esen, C.; Garcia-Cruz, A.; Piletsky, S. A. Molecularly Imprinted Polymers in Electrochemical and Optical Sensors. *Trends Biotechnol.* 2019, 37(3), 294–309. DOI: 10.1016/j.tibtech.2018.08.009.

[20] Rahtuvanoğlu, A.; Akgönüllü, S.; Karacan, S.; Denizli, A. Biomimetic Nanoparticles Based Surface Plasmon Resonance Biosensors for Histamine Detection in Foods. *ChemistrySelect*. 2020, 5(19), 5683–5692. DOI: 10.1002/slct.202000440.

[21] Tancharoen, C.; Sukjee, W.; Thepparit, C.; Jaimipuk, T.; Auewarakul, P.; Thitithanyanont, A.; Sangma, C. Electrochemical Biosensor Based on Surface Imprinting for Zika Virus Detection in Serum. *ACS Sens.* 2019, 4(1), 69–75. DOI: 10.1021/acssensors.8b00885.

[22] Erzengin, M.; Baydemir Peşint, G.; Zenger, O.; Odabaşı, M. Monolithic Hydrophobic Cryogel Columns for Protein Separation. *Polym. Bull.* 2021. DOI: 10.1007/s00289-021-03568-2.

[23] Hixon, K. R.; Lu, T.; Sell, S. A. A Comprehensive Review of Cryogels and Their Roles in Tissue Engineering Applications. *Acta Biomaterialia*. 2017, 62, 29–41. DOI: 10.1016/j.actbio.2017.08.033.

[24] Denizli, A.; Bakhshpour, M.; Akgönüllü, S.; Idil, N.; Yavuz, H.; Andac, M. Versatile Polymeric Cryogels and Their Biomedical Applications. *Hacettepe J. Biol. Chem.* 2020, 48, 99–118. DOI: 10.15671/hjbc.629355.

[25] Bakhshpour, M.; Idil, N.; Perçin, I.; Denizli, A. Biomedical Applications of Polymeric Cryogels. *Appl. Sci*. 2019, 9(3), 1–22. DOI: 10.3390/app9030553.
[26] Pitek, A. S.; O'Connell, D.; Mahon, E.; Monopoli, M. P.; Francesca Baldelli, F.; Dawson, K. A. Transferrin Coated Nanoparticles: Study of the Bionano Interface in Human Plasma. *PLoS One*. 2012, 7(7), e40685. DOI: 10.1371/journal.pone.0040685.
[27] Li, Q.; Yang, K.; Liu, J.; Zhang, L.; Liang, Z.; Zhang, Y. Transferrin Recognition Based on a Protein Imprinted Material Prepared by Hierarchical Imprinting Technique. *Microchim. Acta*. 2013, 180(15–16), 1379–1386. DOI: 10.1007/s00604-013-0994-7.
[28] Saçligil, D.; Şenel, S.; Yavuz, H.; Denizli, A. Purification of Transferrin by Magnetic Immunoaffinity Beads. *J. Sep. Sci*. 2015, 38(15), 2729–2736. DOI: 10.1002/jssc.201500216.
[29] Da Zhang, Y.; Huang, Q. W.; Ma, C.; Liu, X. Y.; Zhang, H. X. Magnetic Fluorescent Molecularly Imprinted Nanoparticles for Detection and Separation of Transferrin in Human Serum. *Talanta*. 2018, 188, 540–545. DOI: 10.1016/j.talanta.2018.06.002.
[30] Zhang, Y.; Cao, H.; Huang, Q.; Liu, X.; Zhang, H. Isolation of Transferrin by Imprinted Nanoparticles with Magnetic Deep Eutectic Solvents as Monomer. *Anal. Bioanal. Chem*. 2018, 410(24), 6237–6245. DOI: 10.1007/s00216-018-1232-2.
[31] Miao, Y.; Sun, X.; Lv, J.; Yan, G. Phosphorescent Mesoporous Surface Imprinting Microspheres: Preparation and Application for Transferrin Recognition from Biological Fluids. *ACS Appl. Mater. Interfaces*. 2019, 11(2), 2264–2272. DOI: 10.1021/acsami.8b17772.
[32] Çetin, K.; Denizli, A. Immunoaffinity Microcryogels for Purification of Transferrin. *J. Chromatogr. B Anal. Technol. Biomed. Life Sci*. 2019, 1114–1115, 5–12. https://doi.org/10.1016/j.jchromb.2019.03.017 .
[33] Çetin, K.; Denizli, A. Microcryogels as Plastic Antibodies for Transferrin Purification. *Process Biochem*. 2019, 79, 174–184. DOI: 10.1016/j.procbio.2018.12.020.
[34] Andaç, M.; Baydemir, G.; Yavuz, H.; Denizli, A. Molecularly Imprinted Composite Cryogel for Albumin Depletion from Human Serum. *J. Mol. Recognit*. 2012, 25(11), 555–563. DOI: 10.1002/jmr.2202.
[35] Baydemir, G.; Denizli, A. Heparin Removal from Human Plasma Using Molecular Imprinted Cryogels. *Artif. Cells Nanomed. Biotechnol*. 2015, 43(6), 403–412. DOI: 10.3109/21691401.2014.897631.
[36] Savina, I. N.; Galaev, I. Y.; Mattiasson, B. Anion-exchange Supermacroporous Monolithic Matrices with Grafted Polymer Brushes of N, N-dimethylaminoethyl-methacrylate. *J. Chromatogr. A*. 2005, 1092(2), 199–205. DOI: 10.1016/j.chroma.2005.06.094.
[37] Baydemir, G.; Bereli, N.; Andaç, M.; Say, R.; Galaev, I. Y.; Denizli, A. Bilirubin Recognition via Molecularly Imprinted Supermacroporous Cryogels. *Colloids Surf. B Biointerfaces*. 2009, 68(1), 33–38. DOI: 10.1016/j.colsurfb.2008.09.008.
[38] Baran, N. Y.; Acet, Ö.; Odabaşı, M. Efficient Adsorption of Hemoglobin from Aqueous Solutions by Hybrid Monolithic Cryogel Column. *Mater. Sci. Eng. C*. 2017, 73, 15–20. DOI: 10.1016/j.msec.2016.12.036.
[39] Aydoğan, C.; Andaç, M.; Bayram, E.; Say, R.; Denizli, A. Molecularly Imprinted Cryogel for L-glutamic Acid Separation. *Biotechnol. Prog*. 2012, 28(2), 459–466. DOI: 10.1002/btpr.1517.
[40] Yıldırım, M.; Baydemir Peşint, G. Molecularly Imprinted Spongy Columns for Angiotensin(II) Recognition from Human Serum. *Biotechnol. Prog*. 2021, 37(2). DOI: 10.1002/btpr.3112.
[41] Le Noir, M.; Plieva, F.; Hey, T.; Guieysse, B.; Mattiasson, B. Macroporous Molecularly Imprinted Polymer/cryogel Composite Systems for the Removal of Endocrine Disrupting Trace Contaminants. *J. Chromatogr. A*. 2007, 1154(1–2), 158–164. DOI: 10.1016/j.chroma.2007.03.064.
[42] Rabieizadeh, M.; Kashefimofrad, S. M.; Naeimpoor, F. Monolithic Molecularly Imprinted Cryogel for Lysozyme Recognition. *J. Sep. Sci*. 2014, 37(20), 2983–2990. DOI: 10.1002/jssc.201400453.
[43] Çetin, K.; Denizli, A. 5-Fluorouracil Delivery from Metal-ion Mediated Molecularly Imprinted Cryogel Discs. *Colloids Surf. B Biointerfaces*. 2015, 126, 401–406. https://doi.org/10.1016/j.colsurfb.2014.12.038.
[44] Bakhshpour, M.; Göktürk, I.; Bereli, N.; Denizli, A. Molecularly Imprinted Cryogel Cartridges for the Selective Recognition of Tyrosine. *Biotechnol. Prog*. 2020, 36(5). DOI: 10.1002/btpr.3006.
[45] Özdaş, S.; Baydemir Peşint, G.; Arısoy, P.; Zenger, O.; Eren, B. Neopterin-Imprinted Columns for Selective Neopterin Recognition from Serum and Urine Samples. *Process Biochem*. 2021, 108, 1–7. DOI: 10.1016/j.procbio.2021.05.022.
[46] Baydemir Peşint, G.; Zenger, O.; Perçin, I.; Denizli, A. Spongy Membranes for Peroxidase Purification from Brassica Oleracea Roots. *Process Biochem*. 2021, 103, 98–106. DOI: 10.1016/j.procbio.2021.02.005.
[47] Odabaşı, M.; Uzun, L.; Baydemir, G.; Aksoy, N. H.; Acet, Ö.; Erdönmez, D. Cholesterol Imprinted Composite Membranes for Selective Cholesterol Recognition from Intestinal Mimicking Solution. *Colloids Surf. B: Biointerfaces*. 2018, 163, 266–274. DOI: 10.1016/j.colsurfb.2017.12.033.
[48] Al-Odayni, A.-B. A.-O.; Saeed, W. S. S.; Ahmed, A. Y. B. H.; Alrahlah, A.; Al-Kahtani, A.; Aouak, T. New Monomer Based on Eugenol Methacrylate, Synthesis, Polymerization and Copolymerization with Methyl Methacrylate–Characterization and Thermal Properties. *Polymers (Basel)*. 2020, 12(1), 2–28. DOI: 10.3390/polym12010160.
[49] Sanches, N. B.; Pedro, R.; Diniz, M. F.; Mattos, E. D. C.; Cassu, S. N.; Dutra, R. D. C. L. Infrared Spectroscopy Applied to Materials Used as Thermal Insulation and Coatings. *J. Aerosp. Technol. Manag*. 2013, 5(4), 421–430. DOI: 10.5028/jatm.v5i4.265.
[50] Neehaul, Y.; Chen, Y.; Werner, C.; Fee, J. A.; Ludwig, B.; Hellwig, P. Electrochemical and Infrared Spectroscopic Analysis of the Interaction of the CuA Domain and Cytochrome C552 from Thermus Thermophilus. *Biochim. Biophys. Acta Bioenerg*. 2012, 1817(10), 1950–1954. DOI: 10.1016/j.bbabio.2012.02.027.

[51] Hawkins, D. M.; Stevenson, D.; Reddy, S. M. Investigation of Protein Imprinting in Hydrogel-based Molecularly Imprinted Polymers (Hydromips). *Anal. Chim. Acta.* 2005, 542(1), 61–65. DOI: 10.1016/j.aca.2005.01.052.

[52] Acet, Ö.; Önal, B.; Sanz, R.; Sanz-Pérez, E. S.; Erdönmez, D.; Odabaşi, M. Preparation of a New Chromatographic Media and Assessment of Some Kinetic and Interaction Parameters for Lysozyme. *J. Mol. Liq.* 2019, 276, 480–487. DOI: 10.1016/j.molliq.2018.12.037.

[53] Alkan, H.; Cömert, Ş. C.; Gürbüz, F.; Doğru, M.; Odabaşı, M. Cu2+-attached Pumice Particles Embedded Composite Cryogels for Protein Purification. *Artif. Cells Nanomed. Biotechnol.* 2017, 45, 90–97. DOI: 10.3109/21691401.2015.1129627.

[54] Baydemir, G.; Andaç, M.; Perçin, I.; Derazshamshir, A.; Denizli, A. Molecularly Imprinted Composite Cryogels for Hemoglobin Depletion from Human Blood. *J. Mol. Recognit.* 2014, 27(9), 528–536. DOI: 10.1002/jmr.2376.

[55] Variyar, P. S.; Chatterjee, S.; Sharma, A. High-performance Thin-layer Chromatography (HPTLC). High-Performance Thin-Layer Chromatogr; 2011: 1–397. DOI: 10.1007/978-3-642-14025-9_2.